ELSEVIER

Journal of Chromatography A, 852 (1999) 507–523

JOURNAL OF CHROMATOGRAPHY A

Gas chromatographic kinetic study of carbon monoxide oxidation over platinum–rhodium alloy catalysts

Dimitrios Gavril, Nicholas A. Katsanos, George Karaiskakis*

Department of Chemistry, University of Patras, GR-26500 Patras, Greece

Received 5 March 1999; received in revised form 18 May 1999; accepted 18 May 1999

Abstract

The kinetics for the oxidation of carbon monoxide in the presence of excess oxygen over Pt–Rh alloy catalysts were studied by using the reversed-flow gas chromatography technique. Suitable mathematical analysis equations were derived by means of which the rate constants for the oxidation reaction of carbon monoxide, as well as for the adsorption and desorption of the reactant CO on the catalysts pure Pt, 75 atom% Pt+25 atom% Rh, 50 atom% Pt+50 atom% Rh, 25 atom% Pt+75 atom% Rh and pure Rh supported on SiO_2 were determined. All the catalysts show a maximum rate constant for the production of CO_2 at a characteristic temperature close to that found in the literature. The rate constants for the adsorption of CO increase generally with increasing temperature, while those for the desorption decrease with increasing temperature. From the variation of the rate constants with temperature activation energies for the oxidation reaction and adsorption of CO were determined, which are sensitive to the composition of the catalytic surface. The appearance of CO_2 and carbon, when introducing pure CO into the column with the catalysts, verified a partial dissociative adsorption (e.g., disproportionation) of CO on the catalysts used. The latter indicates a mechanism for the CO oxidation through a partial dissociative adsorption of CO followed by the reaction of adsorbed CO molecules with adsorbed O atoms.

Keywords: Catalysts; Platinum–rhodium catalysts; Rhodium–platinum catalysts; Kinetic studies; Reversed-flow gas chromatography; Oxidation; Carbon monoxide

1. Introduction

The catalysts for the oxidation of hydrocarbons (C_xH_y) and carbon monoxide (CO) and the reduction of nitrogen oxides (NO_x) in auto exhaust are in an advanced development stage. Most of the converters in gasoline-fueled cars are based on bimetallic platinum–rhodium (Pt–Rh) catalysts which are called three-way catalysts, since the harmful carbon monoxide, nitrogen oxides and hydrocarbons are simultaneously converted into carbon dioxide, nitrogen and water [1]. Despite the widespread use of bimetallic Pt–Rh catalysts and the extensive knowledge about the performance of these catalysts [1–5], little is known about the rate constants of the physicochemical process of adsorption, desorption and surface oxidation reaction of CO, which are important in postulating the mechanism for the CO oxidation [6,7]. Partial solutions to the problem are afforded by static and dynamic chemisorption tech-

*Corresponding author. Tel.: +30-61-997-109/997-144; fax: +30-61-997-118/997-110.

E-mail address: gkaraisk@upatras.gr (G. Karaiskakis)

0021-9673/99/$ – see front matter
PII: S0021-9673(99)00642-1

niques that measure the total number of sites to which an adsorbate bonds, but give no information regarding rate constants and site energetics.

For the kinetic study of the CO oxidation reaction over the Pt–Rh bimetallic catalysts supported on SiO_2, the relatively new technique of reversed-flow gas chromatography (RF-GC) was applied. This offers an alternative route for the measurement of rate constants and the nature of adsorption sites [8].

The RF-GC technique is based on a perturbation imposed on the carrier gas flow by repeatedly reversing its direction for a short time interval. When the carrier gas contains other gases at certain concentrations, recorded by the detector system, the flow reversals create perturbations on the chromatographic elution curve, having the form of narrow and symmetrical extra peaks (''sample peaks''). If the concentration of a constituent in the flowing gas depends on a rate process taking place within a gaseous diffusion column containing a solid bed, then, by repeatedly reversing the flow, one performs a repeated sampling of this rate process. Using suitable mathematical analysis, equations are derived by means of which the rate coefficients of the slow processes responsible for the sample peaks are determined.

RF-GC has been used to determine gas diffusion coefficients in binary and ternary mixtures [9,10], adsorption equilibrium constants [11], molecular diameters and critical volumes in gases [12], Lennard–Jones parameters [13], activity coefficients [14], mass transfer coefficients on solids and liquids [15–21], solubility and interaction parameters [22], as well as rate constants, activation parameters and conversions of the reactants into products for various important surface-catalysed reactions [23–25].

In the present work the oxidation of carbon monoxide over Pt–Rh alloy catalysts is investigated with the aid of RF-GC. The CO oxidation was chosen because of the well known interest in this reaction in connection with the control of automotive emissions. Moreover it was chosen in order to study the activity for the above reaction of some bimetallic Pt–Rh catalysts synthesized and well characterized by various techniques in the Leiden Laboratory [2]. Rate constants and activation parameters for the oxidation of CO over Co_3O_4 containing catalysts were also determined in a previous work [23] by using the RF-GC technique. The reason for studying again this reaction by RF-GC, apart from the fact that we use new Pt–Rh bimetallic catalysts, is the development of an advanced theoretical treatment, which allows us to determine, not only the rate constants for the oxidation reaction, but also the rate constants for the adsorption and desorption of CO on the catalysts used.

2. Experimental

2.1. Materials

The catalysts used were pure Pt and Rh supported on SiO_2 (3%, w/w), as well as $Pt_{0.75}$–$Rh_{0.25}$, $Pt_{0.50}$–$Rh_{0.50}$ and $Pt_{0.25}$–$Rh_{0.75}$ alloys supported also on SiO_2 (3%, w/w). The method of preparation and the surface characterization of the catalysts using thermal desorption spectroscopy (TDS) and X-ray photoelectron spectrometry (XPS) have been presented previously [2,3]. Before use, the catalysts were reduced at 628 K for 10 h in flowing hydrogen at a flow-rate of 1.0 ml s^{-1}.

Carbon monoxide from Linde (99.97% pure) was used as reactant, while the product carbon dioxide was identified by using CO_2 (99.97% pure) from Matheson Gas Products.

The carrier gas was a mixture of 93% (v/v) helium (of purity 99.999%) and 7% (v/v) oxygen (99.999% pure) from BOC Gases, while the hydrogen used for the reduction of the catalysts was purchased from Linde (99.999% pure).

The chromatographic material was silica gel 80–100 mesh from Supelco.

2.2. Apparatus

The experimental set-up, which has been described in detail elsewhere [20,21] is shown in Fig. 1. A conventional gas chromatograph (Shimadzu 8A) contained in its oven (Fig. 1, oven 1) two sections of lengths l' and l of a stainless steel chromatographic column [(38+38) cm×4 mm I.D.] containing no chromatographic material. A stainless steel diffusion column of length L (117.6 cm×4 mm I.D.) was connected perpendicularly at its lower end to the middle of the column $l'+l$ and was empty of any

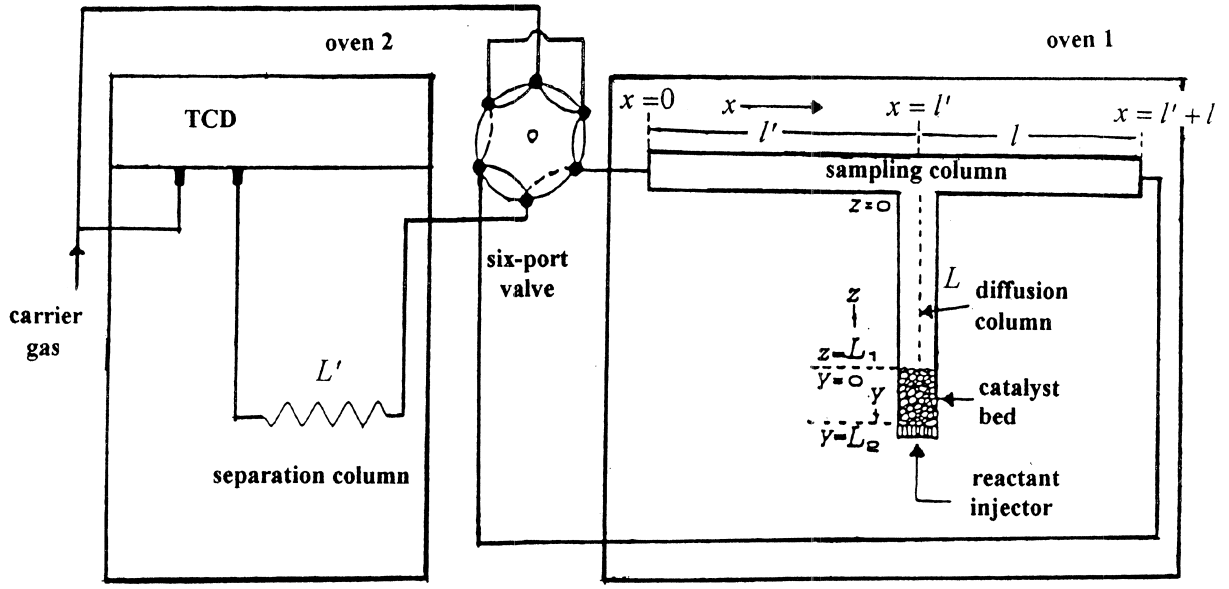

Fig. 1. Experimental set-up for the kinetic study of carbon monoxide oxidation over Pt–Rh alloy catalysts by reversed-flow gas chromatography.

solid or liquid material, except for a short length (~1.0 cm) at the upper end, which contained the catalyst (0.09–0.18 g). The one end of the sampling column $l'+l$ was connected, via a six-port valve, to the carrier gas supply [a mixture of He (93%, v/v) and O_2 (7%, v/v)], while the other end was connected to the separation column of length L', which was placed in oven 2 of another gas chromatograph (Pye-Unicam Series 104). The end of this column was connected to the thermal conductivity detection (TCD) system, as shown. The length of the separation column, which was packed with silica gel 80–100 mesh (7.6 g), was 45 cm, while its internal diameter was 4 mm.

2.3. Procedure

Before measurements, the whole system was conditioned by heating in situ the catalyst at 743 K and the silica gel at 423 K both for 20 h, under carrier gas (93%, v/v, He+7%, v/v, O_2) flow. Some preliminary injections of the reactant carbon monoxide were made to stabilise the catalysts, and then, with the carrier gas flowing in direction from $x = 0$ to $x = l' + l$ (cf. Fig. 1) with a flow-rate of 1.0 ml s^{-1}, 1 ml of carbon monoxide under atmospheric pressure was rapidly introduced with a gas-tight syringe at the top of the diffusion column L. After some time (usually about 10 min), a continuous concentration–time curve decreasing slowly is established in the recorder owing to both the reactant CO and the product CO_2. During this period, reversals of the carrier gas flow-direction for 5 s were made, and then the gas was again turned to its original direction, by simply switching the six-port valve from one position to the other, and vice versa. This time period was shorter than the gas hold-up time in column sections l', l and L'. When the gas flow was restored to its original direction, two sample peaks were recorded (cf. Fig. 2). The first peak belonged to the reactant CO and the second to the product CO_2. The above flow reversal procedure was repeated many times at each temperature, giving rise to two series of sample peaks (one for CO and one for CO_2), each pair of peaks corresponding to a different time from the reactant injection. This means that one can easily make many measurements of the catalytic activity at the catalyst's steady state.

The pressure drop along the whole system was 0.33 atm (1 atm = 101 325 Pa). The working temperature range was 553–748 K for the catalyst bed (oven 1), while it was kept constant at 358 K for the

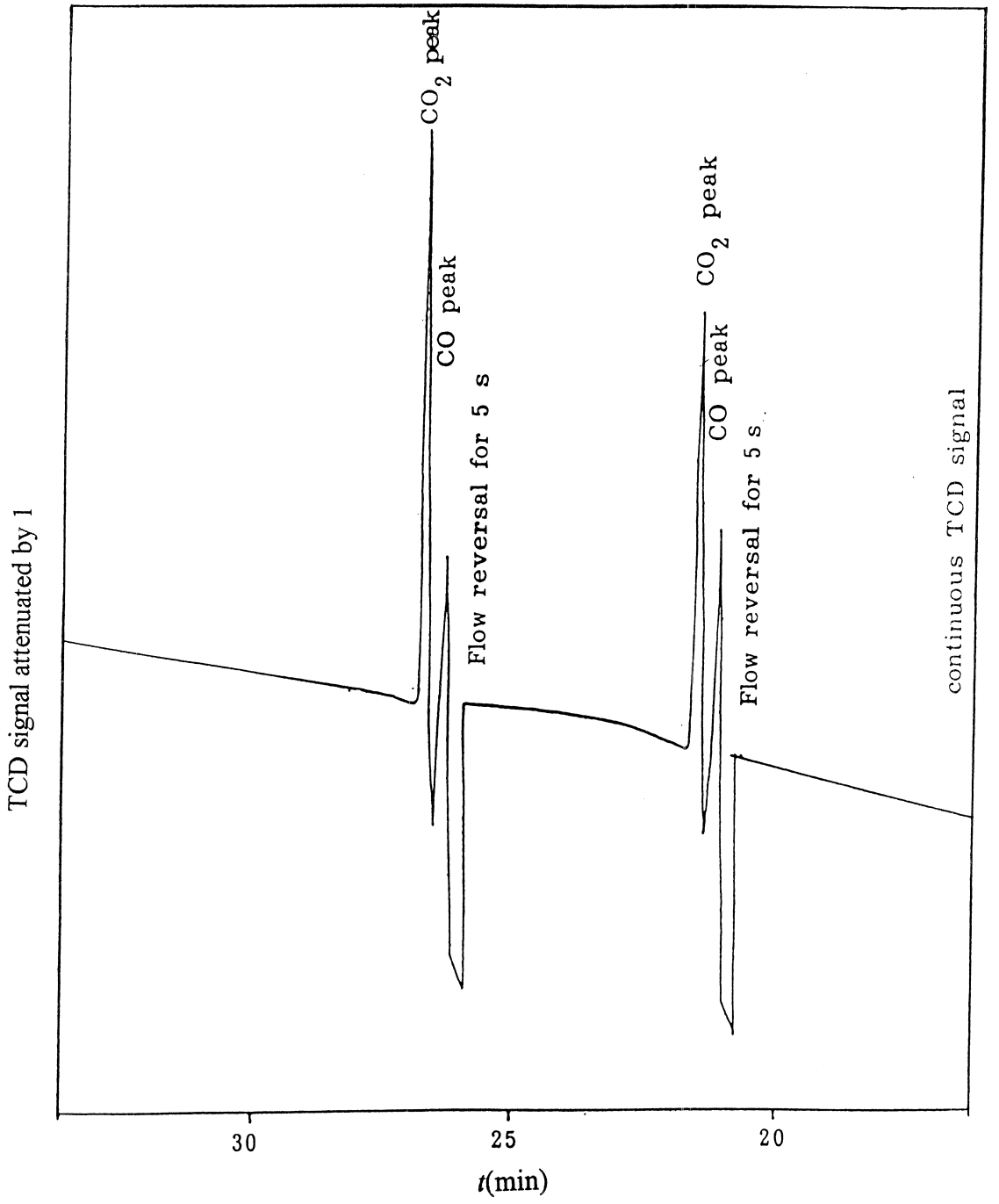

Fig. 2. Reversed-flow chromatogram showing two sample peaks for the reactant CO (first peak) and the product CO_2 (second peak) for the experiments done with decreasing temperature ($T=613$ K) in the presence of the catalyst $Pt_{0.75}+Rh_{0.25}$.

chromatographic material (oven 2). The variations in the temperature along the catalytic bed, which were measured by a digital thermometer Fluke 2190A, were smaller than 1 K. The volumetric carrier gas flow-rate at ambient temperature was 1.0 ml s^{-1}.

3. Theory

The height H of the extra chromatographic peaks, obtained by repeated flow reversals, is proportional to the concentration $c(l', t)$ at the point $x=l'$ and at time t:

$$H^{1/M} = gc(l', t) \tag{1}$$

where M is the response factor of the detector and g the proportionality constant, which can be determined as described elsewhere [26].

If ln H is plotted against t for each substance, a so-called ''diffusion band'' is obtained, like that of Fig. 3. The mathematical equation describing the diffusion band of the reactant in the presence of catalyst is the following [27,28]:

$$H^{1/M} = A_1 \exp(B_1 t) + A_2 \exp(B_2 t) + A_3 \exp(B_3 t) + A_4 \exp(B_4 t) \tag{2}$$

where the pre-exponential factors A_1, A_2, A_3 and A_4 are explicit functions of various physicochemical quantities including m (the injected amount of reactant in mol), B_1, B_2, B_3, B_4, k_{-1} and k_2, the analytical form of which are not needed. The exponential coefficients of time B_1, B_2, B_3 and B_4 satisfy the following equations:

$$X = \alpha_2(1+V_1) + k_{-1} + k_2 = -(B_1 + B_2 + B_3 + B_4) \tag{3}$$

$$Y = [\alpha_2(1+V_1)](k_{-1}+k_2) + \alpha_1\alpha_2 + k_1k_{-1} = B_1B_2 + B_1B_3 + B_1B_4 + B_2B_3 + B_2B_4 + B_3B_4 \tag{4}$$

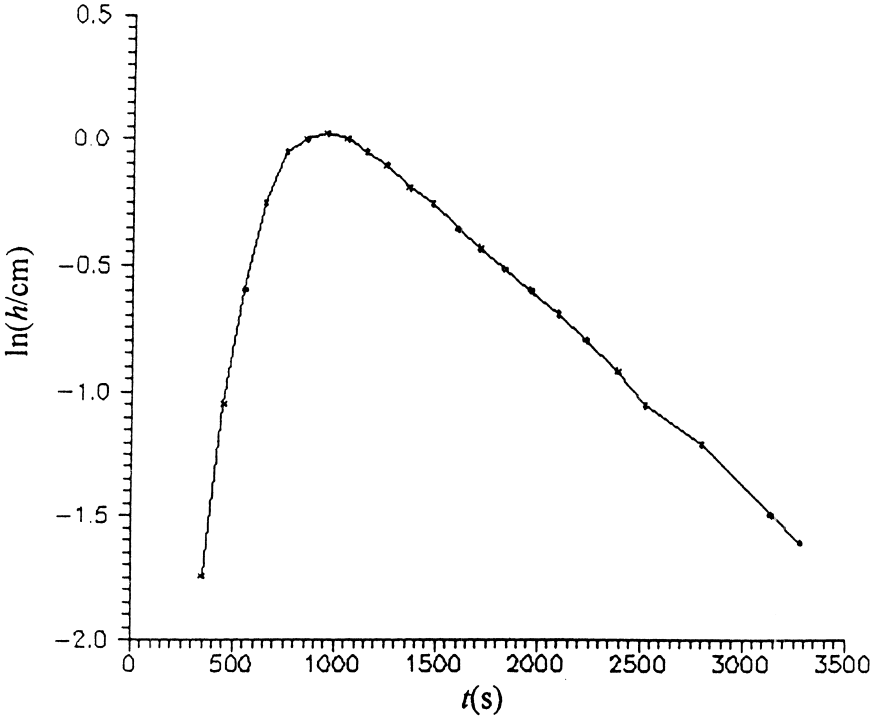

Fig. 3. Example of plotting the diffusion band (ln H vs. t) of the reactant carbon monoxide for the experiments done with decreasing temperature ($T=613$ K) in the presence of the catalyst $Pt_{0.75}+Rh_{0.25}$.

$$Z = \alpha_1\alpha_2(k_{-1}+k_2) + \alpha_2 V_1 k_1 k_{-1} + k_1 k_{-1} k_2 = -(B_1B_2B_3 + B_1B_2B_4 + B_1B_3B_4 + B_2B_3B_4) \quad (5)$$

$$W = \alpha_2 V_1 k_1 k_{-1} k_2 = B_1B_2B_3B_4 \quad (6)$$

In the previous equations $a_1 = 2D_1/L_1^2$, $a_2 = 2D_2/L_2^2$, D_1 is the diffusion coefficient of the reactant into the carrier gas in the column L_1 (see Fig. 1), while D_2 is the diffusion coefficient of the same system in the column L_2 (see Fig. 1), k_1 is the dynamic rate constant for the adsorption of the reactant CO on the catalysts (s^{-1}), k_{-1} is the rate constant for the desorption of the reactant from the bulk solid catalyst (s^{-1}), k_2 is the rate constant (s^{-1}) of a possible first-order or pseudo first-order surface reaction of the adsorbed carbon monoxide molecules and oxygen atoms, and the volume ratio V_1 is given by the relation [28]

$$V_1 = \frac{2V'_G(\text{empty})\epsilon}{V_G} + \frac{L_2^2}{L_1^2} \quad (7)$$

where V_G and V'_G are the gaseous volumes of empty sections L_1 and L_2, respectively (see Fig. 1) and ϵ is the external porosity of the catalyst.

In order that diffusion coefficients in calculating α_1 and α_2 are not obtained from other sources, one can use a steady state approximation for the adsorbed reactant concentration [27,28], leading to the following sum of three exponential functions of time for H, instead of four as in Eq. (2):

$$H^{1/M} = A_5 \exp(B_5 t) + A_6 \exp(B_6 t) + A_7 \exp(B_7 t) \quad (8)$$

where A_5, A_6 and A_7, as A_1, A_2, A_3 and A_4 of Eq. (2), are given by expressions independent of time, while the exponential functions B_5, B_6 and B_7 satisfy the following relations:

$$X_1 = \alpha_2(1+V_1) = -(B_5 + B_6 + B_7) \quad (9)$$

$$Y_1 = \alpha_1\alpha_2 + \frac{k_1 k_{-1} k_2}{k_{-1}+k_2} = B_5B_6 + B_5B_7 + B_6B_7 \quad (10)$$

$$Z_1 = \frac{\alpha_2 V_1 k_1 k_{-1} k_2}{k_{-1}+k_2} = -(B_5B_6B_7) \quad (11)$$

Using a suitable personal computer programme [28], one can calculate the exponential coefficients of time B_1, B_2, B_3 and B_4 of Eq. (2), as well as the coefficients B_5, B_6 and B_7 of Eq. (8), from the experimental points of H (the height of the sample peaks in arbitrary units) and t (the respective times when the flow reversals were made).

From the known values of B_1, B_2, B_3, B_4, B_5, B_6 and B_7, one can calculate the auxiliary parameters X, Y, Z, W, X_1, Y_1 and Z_1, by using Eqs. (3)–(6) and (9)–(11). From the ratio W/Z_1 or the difference $X - X_1$ the sum $k_{-1}+k_2$ is obtained, while the value of $a_2(1+V_1)$ is calculated by subtraction of $k_{-1}+k_2$ from X. The value of a_2V_1 is computed from $a_2(1+V_1)$, since V_1 is known from the geometric characteristics of the cell. Combination of Eqs. (4)–(6) gives the following relation from which the product k_1k_{-1} can be calculated.

$$k_1k_{-1} = \left\{ Y - [\alpha_2(1+V_1)](k_{-1}+k_2) - \frac{Z}{k_{-1}+k_2} + \frac{W}{\alpha_2 V_1 (k_{-1}+k_2)} \right\} \Big/ \left(1 - \frac{\alpha_2 V_1}{k_{-1}+k_2}\right) \quad (12)$$

Dividing W by a_2V_1 the factor $k_1k_{-1}k_2$ can be calculated, from which the k_2 value can be computed, since the product k_1k_{-1} has been already determined from Eq. (12). The value of k_{-1} results from the difference $(k_{-1}+k_2)-k_2$ and that of k_1 from the ratio k_1k_{-1}/k_{-1}.

4. Results and discussion

Rate constants for the adsorption (k_1) and desorption (k_{-1}), as well as for the oxidation reaction of carbon monoxide (k_2) on all catalysts used and at various temperatures were calculated using the procedure described in the theoretical section. The variation of the rate constants with temperature, which is shown in Figs. 4 and 5, indicates that the rate constants for the adsorption increase generally with increasing temperature, while those for the desorption decrease with increasing temperature. On the other hand the rate constants for the oxidation reaction show a maximum at a characteristic temperature T_m depending on the surface composition of the catalyst. The T_m values, which were calculated

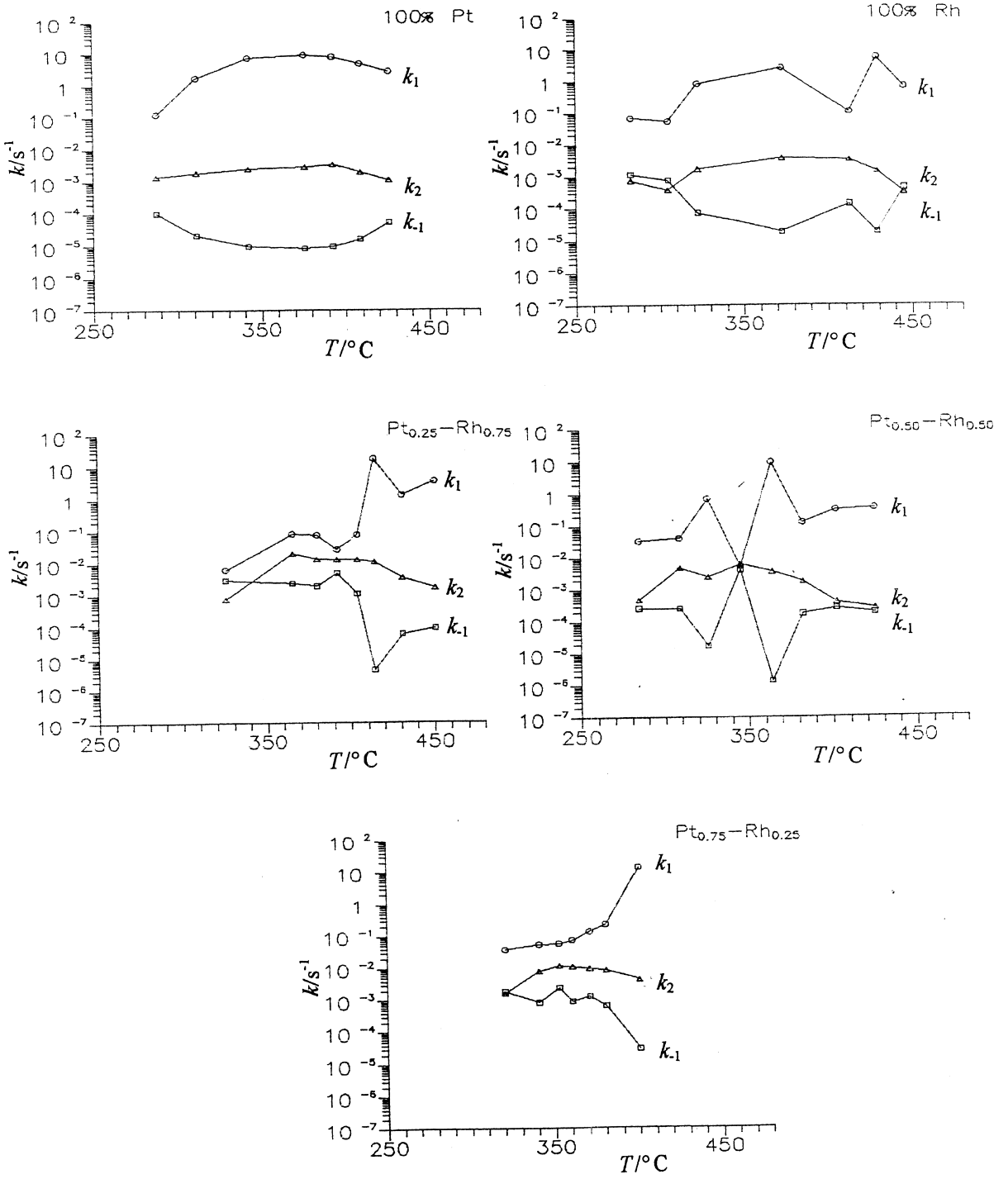

Fig. 4. Variation of the rate constants for the adsorption (k_1), desorption (k_{-1}) and oxidation reaction of CO (k_2) with temperature, for experiments done with increasing temperature over the supported on SiO_2 catalysts shown in the scheme.

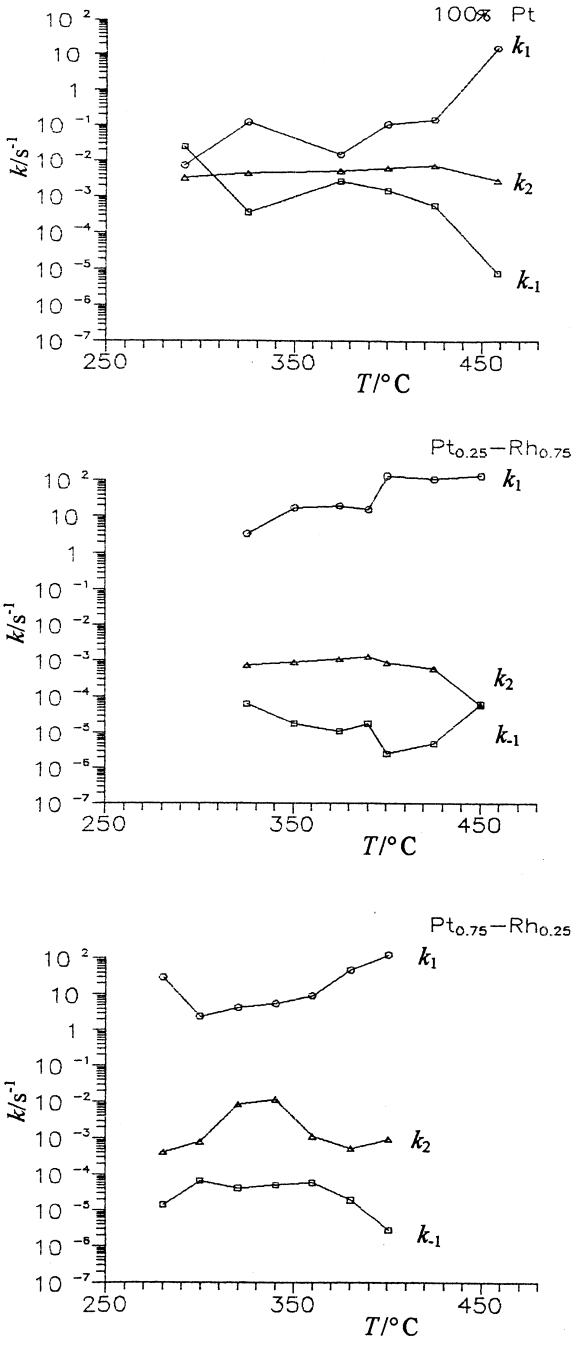

Fig. 5. Temperature dependence of k_1, k_{-1} and k_2 for the CO oxidation reaction over the supported on SiO_2 catalysts shown in the scheme for experiments done with decreasing temperature.

Table 1
Characteristic temperatures for maximum rate constants for the oxidation reaction of CO, over Pt–Rh alloy catalysts, for increasing (T_{m1}) and decreasing (T_{m2}) temperature vs. the catalyst Pt content (at % Pt)

At % Pt	T_{m1} (K)	T_{m2} (K)
0	670	–
25	659	653
50	623	–
75	618	613
100	665	693

by a computer programme, for increasing and decreasing temperature are compiled in Table 1. The experimental data are consistent with previous results [2,3], in which a temperature of maximum carbon dioxide production over the Pt–Rh bimetallic catalysts was also observed. The T_m values found in the present work (618 K and 613 K for increasing and decreasing temperature, respectively, for the catalyst $Pt_{0.75}$–$Rh_{0.25}$ and 659 K and 653 K for increasing and decreasing temperature, respectively, for the catalyst $Pt_{0.25}$–$Rh_{0.75}$) are in good agreement with the corresponding temperature values of 615 K and 665 K for the maximum CO_2 production presented previously [2,3]. Apparently the surface composition has a significant influence on T_m. This can be explained either on the basis of the metal–oxygen bond strength, which is weaker for Pt than for Rh or on the Pt–Rh synergism [4,29] in the bimetallic catalysts, which has a different effect on the catalysts depending on the surface composition.

We conducted some experiments to investigate how the extent of the synergistic effect depends on the composition of the bimetallic catalyst. Fig. 6 shows the characteristic temperature T_m for maximum rate constant for the oxidation reaction of CO as a function of the atomic percentage of Pt for increasing and decreasing temperature (with the total number of noble metal atoms in the catalyst sample held constant). Fig. 6 shows that the characteristic temperature for the maximum rate constant of CO oxidation goes through a minimum as the Pt content in the catalyst increases, indicating the presence of beneficial Pt–Rh synergism over the wide catalyst composition range considered.

For reference purposes the data for the Pt-only and Rh-only catalysts are also included in Fig. 6. Fig. 6

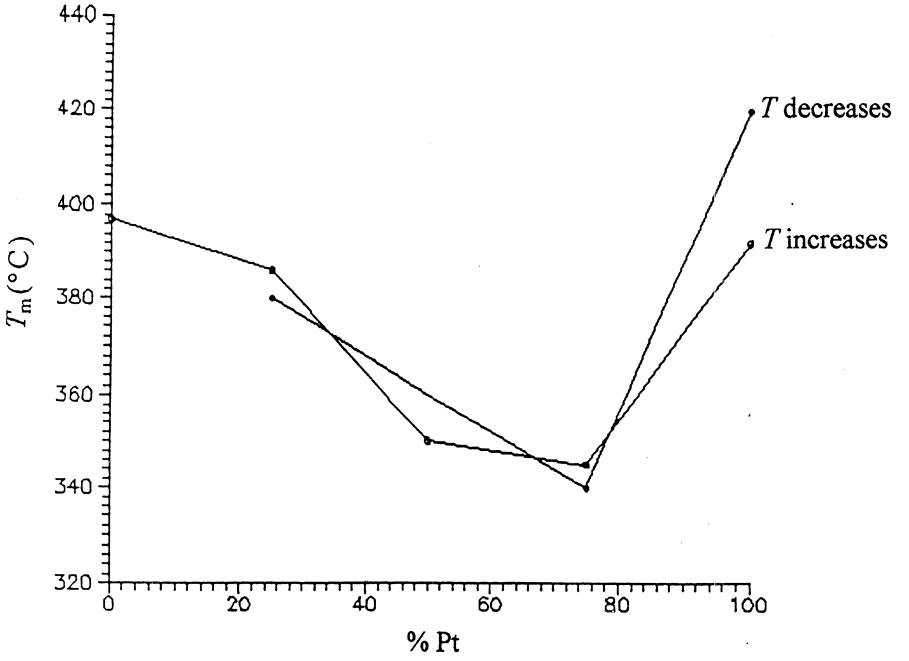

Fig. 6. Variation of the characteristic temperature T_m for maximum rate constant for the oxidation reaction of CO over Pt–Rh bimetallic catalysts with the atomic percentage of Pt for increasing and decreasing temperature.

is in absolute agreement with Fig. 4 of Ref. [4], in which the temperature for 50% CO conversion was presented as a function of catalyst composition. From Fig. 6 the following conclusions for the oxidation reaction of CO over the Rt–Rh catalysts can be extracted:

(i) The characteristic temperature of the maximum rate constant for the experiments done with increasing temperature, which is a measure of the catalytic activity, follows the order: $T_m(Pt_{0.75}–Rh_{0.25})< T_m(Pt_{0.50}–Rh_{0.50})<T_m(Pt_{0.25}–Rh_{0.75})<T_m$(pure Pt)- $<T_m$(pure Rh).

The corresponding T_m values for the experiments done with decreasing temperature follow the order: $T_m(Pt_{0.75}–Rh_{0.25})<T_m(Pt_{0.25}–Rh_{0.75})<T_m$(pure Pt).

(ii) The maximum T_m temperature for the experiments conducted with increasing temperature on the pure Rh can be attributed to the well known formation of the inactive oxide Rh_2O_3, which suppresses CO chemisorption significantly [30,31]. So, the Rh-only catalyst exhibits relatively low CO oxidation activity under the net-oxidizing conditions used in the present work.

(iii) The T_m temperature for the Pt-only catalyst with increasing temperature is also higher than those for the bimetallic catalysts, because the Pt surface is predominantly covered with CO, leaving very little active sites for oxygen adsorption.

(iv) The Pt–Rh synergism in the bimetallic catalysts increases gradually with increasing Pt content, as the T_m temperature decreases with increasing Pt content. Thus, a synergistic enhancement of CO oxidation activity is observed over the Pt–Rh bimetallic catalysts. This can be attributed to the fact that Pt (CO source) and Rh (oxygen source) are randomly distributed on the surface increasing the probability of finding surface CO and oxygen in the vicinity of each other. The increased catalytic activity with increasing Pt suggests that the Pt in the bimetallic catalyst directly participates in the oxidation reaction.

(v) The temperatures for the maximum rate constant of the CO oxidation over the bimetallic catalysts used are lower for the experiments done with decreasing temperature compared to those obtained under the same experimental conditions but with increasing temperature. The latter, which is in accord with previous results [2], indicates that the

surface composition and hence the catalytic activity is dependent on the initial equilibration temperature. On the other hand for the pure Pt catalyst the characteristic temperature for maximum rate constant of the CO oxidation is higher in the case when the temperature decreases. This can be attributed to the inhibited action of CO, which at high temperatures is selectively adsorbed on the pure Pt.

From the variation of the rate constants k_1 and k_2 with temperature, the activation energies for the adsorption, E_{a1}, and oxidation reaction, E_{a2}, of CO were determined for increasing and decreasing temperature (cf. the Arrhenius plots in Figs. 7–10). Since the rate constant k_2 is kinetically controlled at temperatures lower than the characteristic temperature T_m, while at higher temperatures the product composition is controlled by an equilibrium between CO and CO_2, the Arrhenius equation for k_2 was applied at temperatures lower than T_m. From the activation energies presented in Tables 2 and 3 and their variation with the catalyst Pt content shown in Figs. 11 and 12 the following conclusions can be drawn:

(i) The activation energies for the adsorption of CO on the catalysts used range between 57 and 172 kJ mol^{-1}, indicating a process of chemisorption.

(ii) The activation energies for the adsorption of CO on the Pt–Rh bimetallic catalysts for both series of experiments done with increasing and decreasing temperature, decrease with increasing the catalyst Pt content.

(iii) The activation energies for the oxidation reaction of CO over the Pt–Rh alloy catalysts decrease with increasing the Pt content. The latter which can be attributed to synergetic effects is in agreement with the variation of the characteristic temperature for the maximum rate constant k_2 with the Pt content presented in Fig. 6.

(iv) The lower activation energies for the oxidation reaction of CO, which were found for the experiments done with decreasing temperature compared to those with increasing temperature, can be attributed to the catalyst pretreatment, which, as it was pointed out previously, influences strongly the catalytic activity. Such unexpected low values of activation energies for the oxidation reaction of CO over bimetallic catalysts have been also presented previously [31].

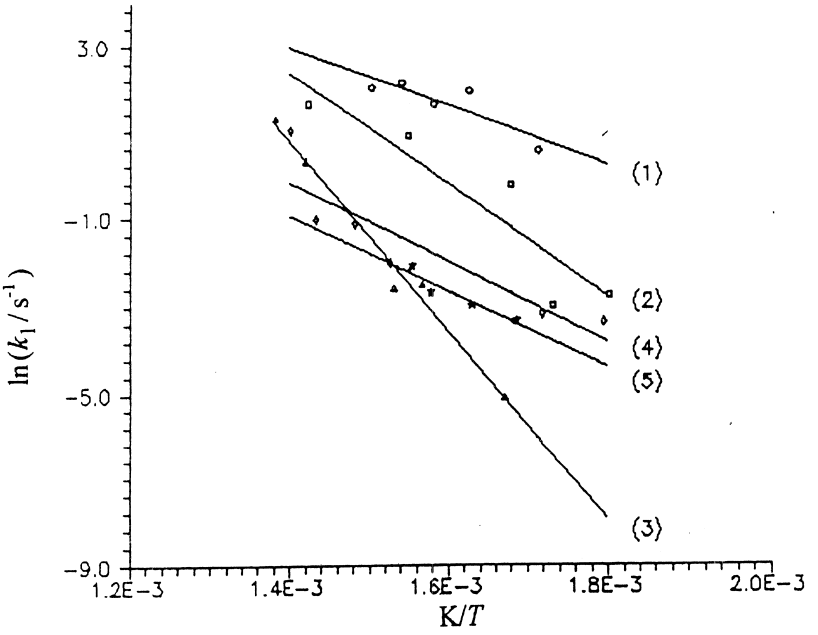

Fig. 7. Arrhenius plots for the adsorption of CO on the Pt–Rh alloy catalysts with increasing temperature. (1) Pt_{pure}; (2) Rh_{pure}; (3) $Pt_{0.25}+Rh_{0.75}$; (4) $Pt_{0.50}+Rh_{0.50}$; (5) $Pt_{0.75}+Rh_{0.25}$.

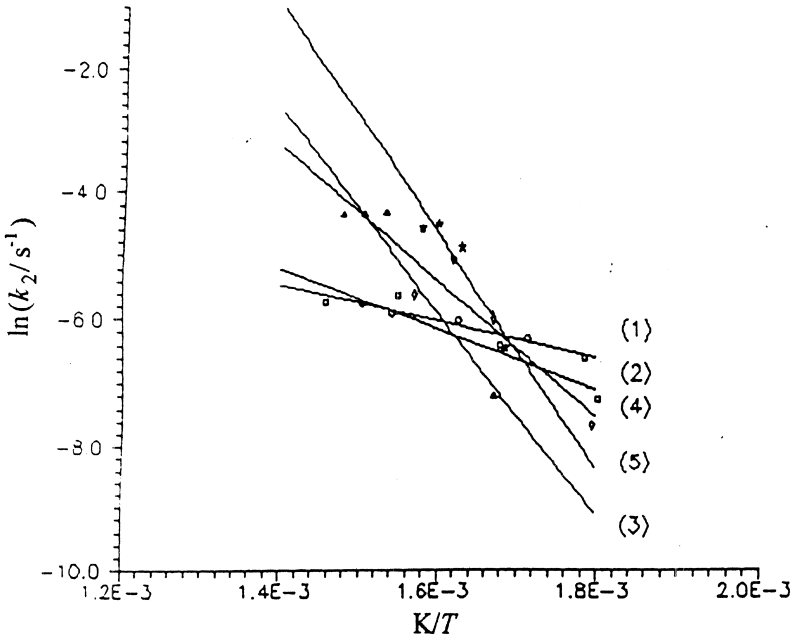

Fig. 8. Arrhenius plots for the oxidation of CO over the Rt–Rh alloy catalysts with increasing temperature. (1) Pt_{pure}; (2) Rh_{pure}; (3) $Pt_{0.25}+Rh_{0.75}$; (4) $Pt_{0.50}+Rh_{0.50}$; (5) $Pt_{0.75}+Rh_{0.25}$.

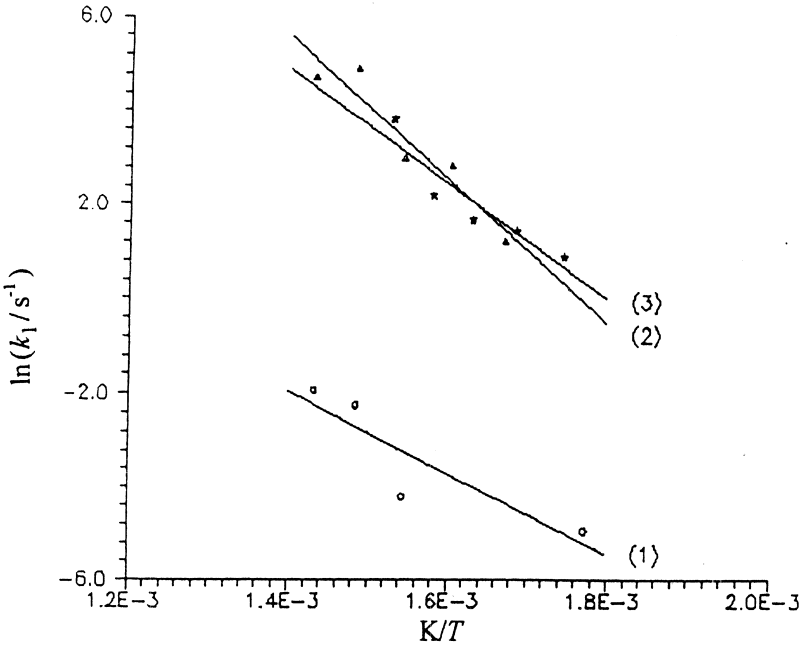

Fig. 9. Arrhenius plots for the adsorption of CO on the Pt–Rh alloy catalysts with decreasing temperature. (1) Pt_{pure}; (2) $Pt_{0.25}+Rh_{0.75}$; (3) $Pt_{0.75}+Rh_{0.25}$.

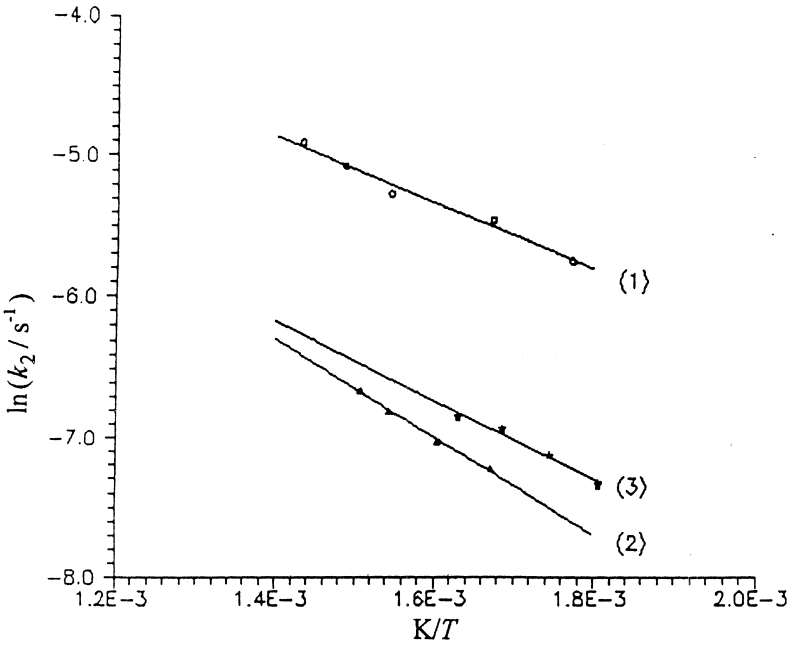

Fig. 10. Arrhenius plots for the oxidation of CO over the Pt–Rh alloy catalysts with decreasing temperature. (1) Pt_{pure}; (2) $Pt_{0.25}+Rh_{0.75}$; (3) $Pt_{0.75}+Rh_{0.25}$.

Table 2
Activation energies for the adsorption of CO on various Pt–Rh alloy catalysts for increasing ($E_{a1}^{dec.}$) and decreasing ($E_{a1}^{dec.}$) temperature

At % Pt	$E_{a1}^{inc.}$ (kJ mol^{-1})	$E_{a1}^{dec.}$ (kJ mol^{-1})
0	108±26[a]	–
25	172±37	127±24
50	76±18	–
75	69±18	102±24
100	57±19	73±27

[a] The ± values are standard errors.

Table 3
Activation energies for the oxidation reaction of CO over Pt–Rh alloy catalysts as a function of the catalyst Pt content for increasing ($E_{a2}^{inc.}$) and decreasing ($E_{a2}^{dec.}$) temperature

At % Pt	$E_{a2}^{inc.}$ (kJ mol^{-1})	$E_{a2}^{dec.}$ (kJ mol^{-1})
0	65±30[a]	–
25	133±25	29±1
50	88±28	–
75	53±34	23±3
100	39±9	20±2

[a] The ± values are standard errors.

The only physicochemical assumptions concerning the gas/solid interactions are that all parameters measured directly or calculated indirectly refer to elementary steps at equilibrium. Based on that, the ratio k_1/k_{-1} with the real experimental isotherm used in the derivation of the relevant equations [27,28] represent equilibrium constants K, according to the principle of microscopic reversibility. It was not an easy thing before to measure simultaneously rate constants of adsorption (k_1) and desorption (k_{-1}) at a dynamic equilibrium state like that justified experimentally in our experiments. The variation of the adsorption constants $K=k_1/k_{-1}$ with temperature, shown in Figs. 13 and 14, gives the apparent standard molar internal energy change $\Delta U^0_{app.}$, which may be the standard molar internal energy change $\Delta U^0_{co.}$ in the adsorption process of the reactant CO or the difference $\Delta U^0_{co.}-\Delta U^0_c$, where ΔU^0_c is the standard molar change in internal energy when an inhibitor is adsorbed, covering a much bigger fraction of the active surface compared to that covered by the reactant CO. Since ΔU^0_c is negative the total equilibrium energy of adsorption $\Delta U^0_{co.}-\Delta U^0_c$ in the second case may be positive. Taking into considera-

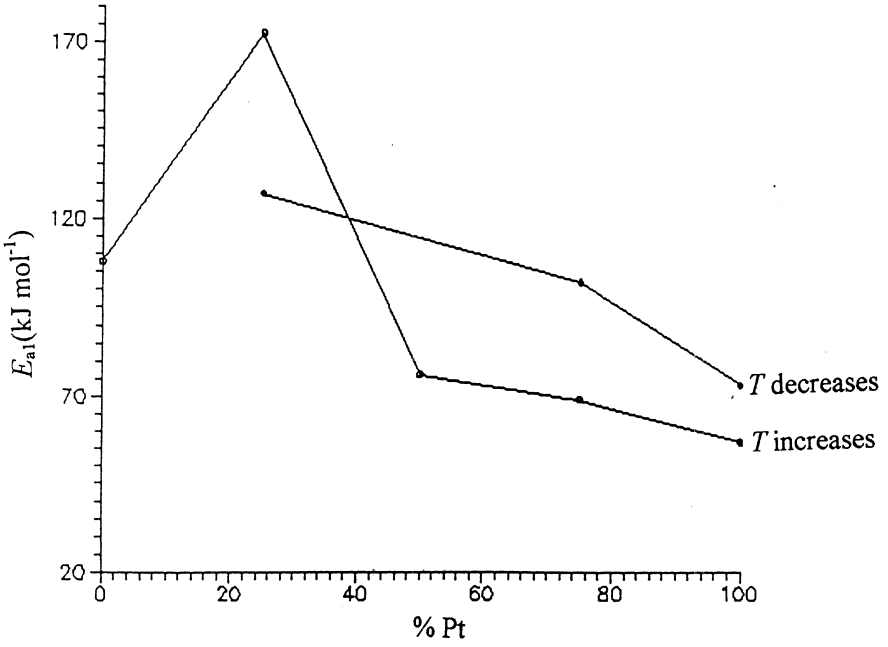

Fig. 11. Plot of the activation energy E_{a1} for the adsorption of CO on the Pt–Rh alloy catalysts vs. the Pt content for increasing and decreasing temperature.

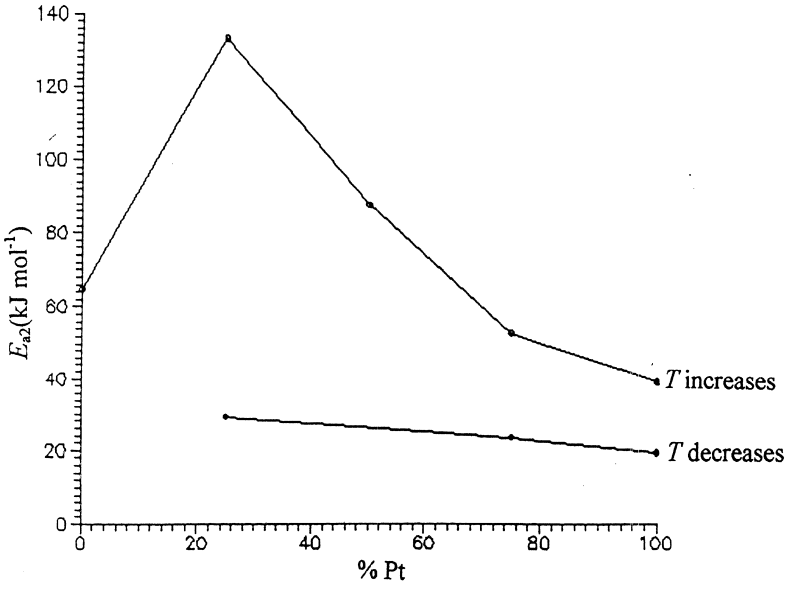

Fig. 12. Plot of the activation energy E_{a2} for the oxidation reaction of CO over the Pt–Rh alloy catalysts vs. the Pt content for increasing and decreasing temperature.

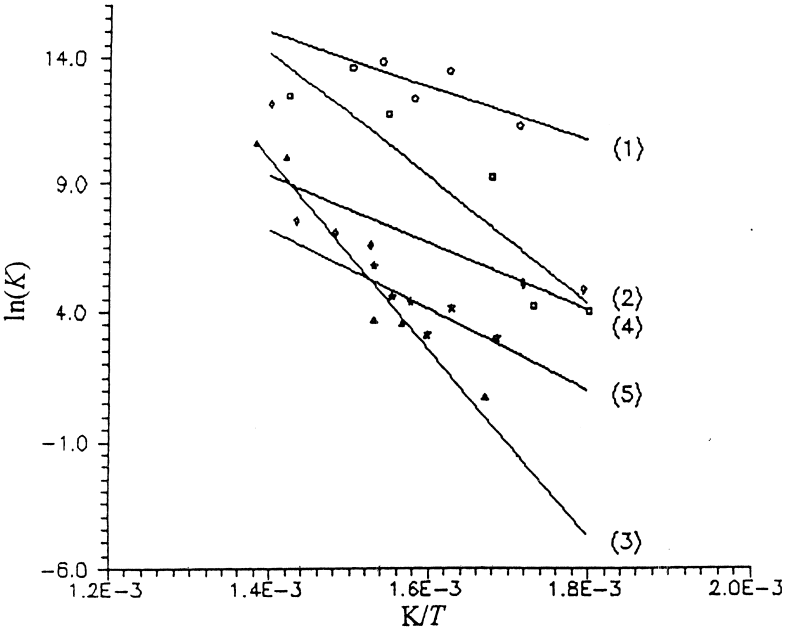

Fig. 13. Van 't Hoff plots for the adsorption of CO on the Pt–Rh alloy catalysts with increasing temperature. (1) Pt_{pure}; (2) Rh_{pure}; (3) $Pt_{0.25}+Rh_{0.75}$; (4) $Pt_{0.50}+Rh_{0.50}$; (5) $Pt_{0.75}+Rh_{0.25}$.

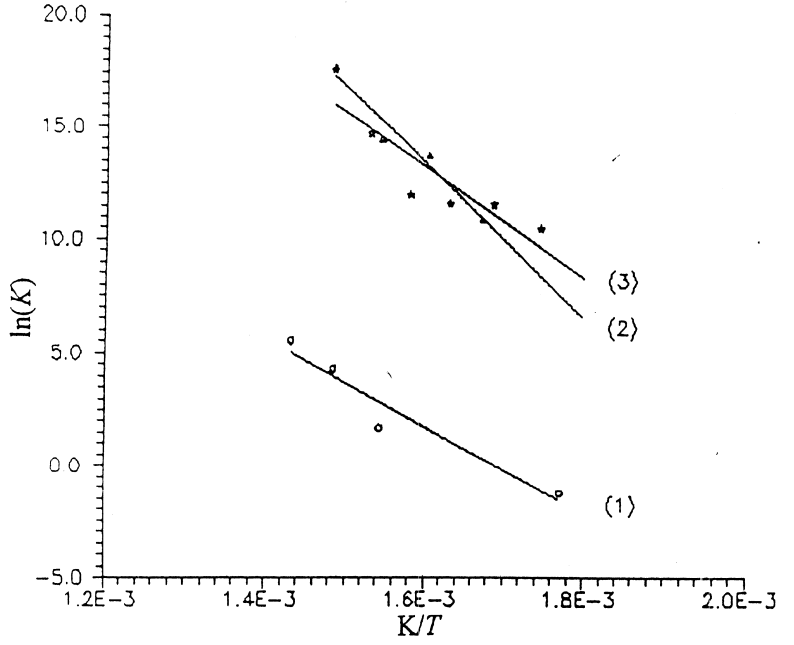

Fig. 14. Van 't Hoff plots for the adsorption of CO on the Pt–Rh alloy catalysts with decreasing temperature. (1) Pt_{pure}; (2) $Pt_{0.25}+Rh_{0.75}$; (3) $Pt_{0.75}+Rh_{0.25}$.

Table 4
Apparent, $\Delta U^0_{app.}$ (kJ mol^{-1}) $= \Delta U^0_{co.} - \Delta U^0_c$ and true, $\Delta U^0_{co.}$ (kJ mol^{-1}), standard molar internal energy changes for the adsorption of CO on various Pt–Rh alloy catalysts, as well as standard molar changes in internal energy for the adsorption of the inhibitor carbon, ΔU^0_c (kJ mol^{-1}), on the same catalysts for increasing and decreasing temperature

At % Pt	Increasing temperature			Decreasing temperature		
	$\Delta U^0_{app.}$	$\Delta U^0_{co.}$	ΔU^0_c	$\Delta U^0_{app.}$	$\Delta U^0_{co.}$	ΔU^0_c
0	205	−158	−363	–	–	–
25	305	−142	−447	286	−172	−458
50	109	−146	−255	–	–	–
75	98	−131	−229	204	−144	−348
100	89	−155	−244	161	−137	−298

tion that the found values of $\Delta U^0_{app.}$ are positive (cf. Table 4) and the carbon, which, as it will be pointed out later, results from the CO dissociative adsorption, acts as an inhibitor, we can determine the standard molar change in internal energy for the adsorption of carbon as follows:

By using the statistical mechanics relation [32]:

$$K = \frac{h^3 \exp\left(-\Delta U^0_{co.}/RT\right)}{(2\pi m)^{3/2}(kT)^{5/2}} \quad (13)$$

the differential energy of carbon monoxide adsorption, $\Delta U^0_{co.}$, can be calculated. Subtracting $\Delta U^0_{app.} = \Delta U^0_{co.} - \Delta U^0_c$ from the mean value of $\Delta U^0_{co.}$ in the temperature range used to calculate $\Delta U^0_{co.} - \Delta U^0_c$, one can find the value of ΔU^0_c. From the values of standard molar changes in internal energy compiled in Table 4 and the variation of ΔU^0_c with the catalyst Pt content shown in Fig. 15, the following conclusions can be drawn:

(i) The values of $\Delta U^0_{app.}$ are positive due to the reason mentioned earlier.

(ii) The values of ΔU^0_c are negative and large, indicating a spontaneous process of strong carbon chemisorption on the catalysts used.

(iii) Comparison of Figs. 12 and 15 shows that for both experiments done with increasing and decreasing temperature, the activation energy for the oxidation reaction of CO, E_{a2}, increases as the internal energy for the adsorption of the inhibitor carbon decreases. This is reasonable as the deposited on the catalysts carbon inhibits the CO oxidation reaction. The minimum ΔU^0_c value, which shows a strong chemisorption of the inhibitor on the catalytic surface, corresponds to the maximum E_{a2} value, as most of the catalytic active sites are occupied by carbon, which acts as an inhibitor in the CO oxidation reaction.

As far as the CO oxidation mechanism is concerned, it is well established in the literature [2,4] that the primary reaction pathway for the oxidation of CO on noble metals is a surface reaction between adsorbed CO and adsorbed atomic oxygen. Depending on the metal and the temperature, carbon monoxide is either molecularly or dissociatively adsorbed. Dissociative adsorption can lead to the deposition of carbon on the metal surface. Doering et al. [33], Ichikawa et al. [34], as well as Maciejewski and Baiker [35] evidenced the decomposition of CO on small Pd particles deposited on various surfaces, while Ioannides et al. [5] verified the CO dissociation over Rh dispersed on various metal oxides. In the present work we have investigated whether the interaction of CO with the Pt–Rh alloy catalysts leads to its disproportionation by performing a series of experiments under the same experimental conditions as those for the oxidation reaction, but without oxygen in the carrier gas helium. Two chromatographic peaks corresponding to CO and CO_2, as those in the case of CO oxidation in the presence of oxygen, were also obtained, indicating a dissociative adsorption of CO on all the catalysts used. X-Ray diffraction analysis of the catalysts at the end of the kinetic experiments have shown the deposition of carbon on the catalytic surface and verified the disproportionation of CO. Therefore, the most likely mechanism of the carbon monoxide oxidation reaction over the Pt–Rh alloy catalysts used is CO dissociation followed by reaction of adsorbed CO molecules and O(ads) atoms, as follows:

$3CO(g) + 3^* \leftrightarrow 3CO(ads)$

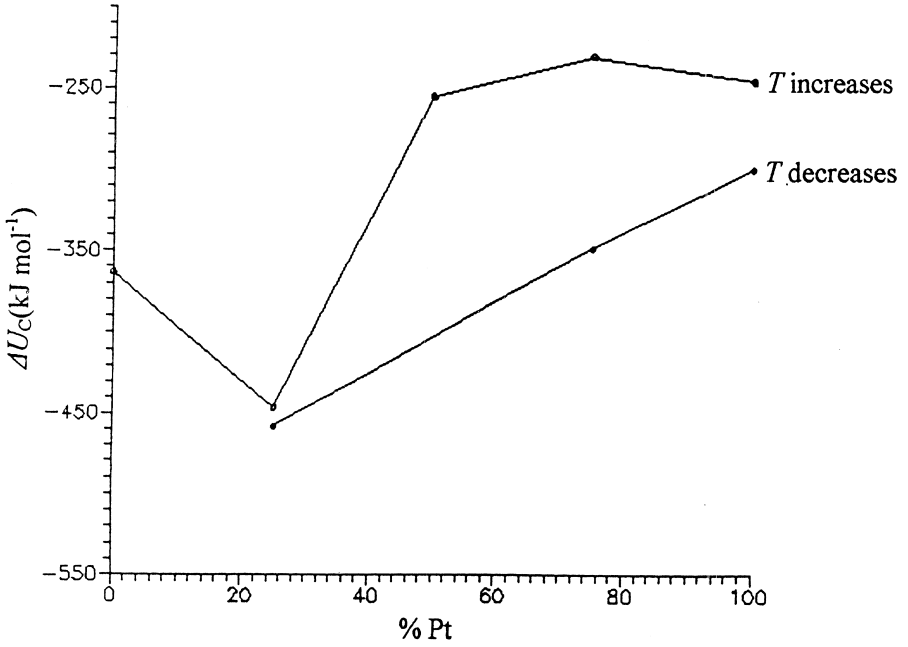

Fig. 15. Variation of the standard molar internal energy change in the adsorption process of carbon, which results from the disssociative adsorption of CO and acts as an inhibitor in the oxidation reaction of CO over the Pt–Rh alloy catalysts, with the atomic percentage of Pt, for increasing and decreasing temperature.

$$CO(ads) + * \rightarrow C(ads) + O(ads)$$

$$O_2(g) + 2* \leftrightarrow 2O(ads)$$

$$3CO(ads) + 3O(ads) \rightarrow 3CO_2(g) + 6*$$

where [*] denotes the number of vacant active sites.

The characteristic temperatures for the maximum rate constants of the CO oxidation found in the present work by the RF-GC technique, considering an apparent first-order reaction order with respect to CO, are in excellent agreement with the temperatures for the maximum rates of CO_2 production presented previously [2,3]. The latter indicates that the hypothesis for a first order reaction with respect to CO is a good approximation under the experimental conditions used (excess of oxygen).

The fact that the derived experimental results which are based on the assumption of a pseudo first-order reaction with respect to carbon monoxide, are consistent with data presented previously [2,3], provides only a necessary, but not a sufficient, condition that the reaction order of the CO oxidation can be approximately considered equal to unity under the experimental conditions used. Obviously, more work is needed under various concentrations of CO in order to investigate the reaction order of the CO oxidation by the reversed-flow gas chromatography technique.

The final conclusion of this study is that the detailed kinetics of carbon monoxide oxidation over Pt–Rh bimetallic catalysts, which is very important for the control of automotive emissions, can be studied with simplicity and accuracy using the relatively new RF-GC technique.

Acknowledgements

The authors thank Dr. Nieuwenhuys at the Leiden University (The Netherlands) for supplying the used catalysts and Mrs. M. Barkoula for technical assistance.

References

[1] F.G. Dwyer, in: H. Heinemann (Ed.), Catalysis Reviews, Vol. 6, Marcel Dekker, New York, 1972, p. 261.
[2] R.M. Wolf, J. Siera, F.C.M.J.M. van Delft, B.E. Nieuwenhuys, Faraday Discuss. Chem. Soc. 87 (1989) 275.
[3] F.C.M.J.M. van Delft, B.E. Nieuwenhuys, J. Siera, R.M. Wolf, ISIJ Int. 29 (1989) 550.
[4] S.H. Oh, J.E. Carpenter, J. Catal. 98 (1986) 178.
[5] T. Ioannides, A.M. Efstathiou, Z.I. Zhang, X.E. Verykios, J. Catal. 156 (1995) 265.
[6] Y.E. Li, D. Willcox, R.D. Gonzallez, AIChE J. 35 (1989) 423.
[7] R.E. Hendershot, R.S. Hansen, J. Catal. 98 (1986) 150.
[8] N.A. Katsanos, G. Karaiskakis, Adv. Chromatogr. 24 (1984) 125.
[9] N.A. Katsanos, G. Karaiskakis, J. Chromatogr. 237 (1982) 1.
[10] G. Karaiskakis, N.A. Katsanos, A. Niotis, Chromatographia 17 (1983) 310.
[11] G. Karaiskakis, N.A. Katsanos, A. Niotis, J. Chromatogr. 245 (1982) 21.
[12] G. Karaiskakis, A. Niotis, N.A. Katsanos, J. Chromatogr. Sci. 22 (1984) 554.
[13] G. Karaiskakis, J. Chromatogr. Sci. 23 (1985) 360.
[14] N.A. Katsanos, G. Karaiskakis, P. Agathonos, J. Chromatogr. 349 (1986) 369.
[15] G. Karaiskakis, N.A. Katsanos, J. Phys. Chem. 88 (1984) 3674.
[16] N.A. Katsanos, E. Dalas, J. Phys. Chem. 91 (1987) 3103.
[17] N.A. Katsanos, P. Agathonos, A. Niotis, J. Phys. Chem. 92 (1988) 1645.
[18] N.A. Katsanos, J. Kapolos, Anal. Chem. 61 (1989) 2231.
[19] A. Koliadima, P. Agathonos, G. Karaiskakis, J. Chromatogr. 550 (1991) 171.
[20] D. Gavril, G. Karaiskakis, Instrum. Sci. Technol. 25 (No. 3) (1998) 217.
[21] D. Gavril, G. Karaiskakis, Chromatographia 47 (1998) 63.
[22] P. Agathonos, G. Karaiskakis, J. Appl. Polym. Sci. 37 (1989) 2237.
[23] G. Karaiskakis, N.A. Katsanos, A. Lycourghiotis, Can. J. Chem. 61 (1983) 1853.
[24] N.A. Katsanos, G. Karaiskakis, A. Niotis, J. Catal. 94 (1985) 376.
[25] E. Dalas, N.A. Katsanos, G. Karaiskakis, J. Chem. Soc., Faraday Trans. I 82 (1986) 2897.
[26] V. Sotiropoulou, G.P. Vassilev, N.A. Katsanos, H. Metaxa, F. Roubani-Kalantzopoulou, J. Chem. Soc., Faraday Trans. I 91 (1995) 485.
[27] Ch. Abatzoglou, E. Iliopoulou, N.A. Katsanos, F. Roubani-Kalantzopoulou, A. Kalantzopoulos, J. Chromatogr. A 775 (1997) 211.
[28] N.A. Katsanos, R. Thede, F. Roubani-Kalantzopoulou, J. Chromatogr. A 795 (1998) 133.
[29] Z. Hu, F.M. Allen, C.Z. Wan, R.M. Heck, J.J. Steger, R.E. Lakis, C.E. Lyman, J. Catal. 174 (1998) 13.
[30] N.K. Pande, A.T. Bell, J. Catal. 98 (1986) 7.
[31] A. Baiker, M. Maciejewski, S. Tagliaferri, P. Hug, J. Catal. 151 (1995) 407.
[32] M. Heuchel, M. Jaroniec, R.K. Gilpin, J. Chromatogr. 628 (1993) 59.
[33] D.L. Doering, H. Poppa, J.T. Dickinson, J. Catal. 73 (1982) 104.
[34] S. Ichikawa, H. Poppa, M. Boudart, J. Catal. 91 (1985) 1.
[35] M. Maciejewski, A. Baiker, J. Phys. Chem. 98 (1994) 285.